Adducts of Oxylipin Electrophiles to Glutathione Reflect a 13 Specificity of the Downstream Lipoxygenase Pathway in the Tobacco Hypersensitive Response

Céline Davoine[1], Olivier Falletti, Thierry Douki, Gilles Iacazio, Najla Ennar, Jean-Luc Montillet, and Christian Triantaphylidès*

Laboratoire de Radiobiologie Végétale, DSV-Département d'Ecophysiologie Végétale et de Microbiologie, CEA-Cadarache, 13108 Saint-Paul Lez Durance cedex, France (C.D., N.E., J.-L.M., C.T.); Laboratoire Lésions des Acides Nucléiques, Service de Chimie Inorganique et Biologique, DSM-Département de Recherche Fondamentale sur la Matière Condensée, Unité Mixte de Recherche-E 3 CEA-UJF, CEA-Grenoble, 38054 Grenoble cedex 9, France (O.F., T.D.); and Laboratoire de Bioinorganique Structurale, Case 432, Unité Mixte de Recherche Centre National de la Recherche Scientifique 6517 Chimie, Biologie et Radicaux libres, Faculté des Sciences de Saint Jérôme, 13397 Marseille cedex 20, France (G.I.)

The response to reactive electrophile species (RES) is now considered as part of the plant response to pathogen and insect attacks. Thanks to a previously established high-performance liquid chromatography tandem mass spectrometry methodology, we have investigated the production of oxylipin RES adducts to glutathione (GSH) during the hypersensitive response (HR) of plants. We have observed that RES conjugation to GSH in tobacco (*Nicotiana tabacum*) leaves is facile and nonspecific. In cryptogein-elicited tobacco leaves, we show that the oxylipin RES adducts to GSH are produced in correlation with GSH consumption, increase in glutathione *S*-transferase activity, and the appearance of the cell death symptoms. In this model, the adducts arise mainly from the downstream 13 lipoxygenase (LOX) metabolism, although the induced 9 LOX pathway leads massively to the accumulation of upstream metabolites. The main adducts were obtained from 2-hexenal and 12-oxo-phytodienoic acid. They accumulate transiently as 1-hexanol-3-GSH, a reduced adduct, and 12-oxo-phytodienoic acid-GSH, respectively. RES conjugation does not initiate cell death but explains part of the GSH depletion that accompanies HR cell death. The nature of these GSH conjugates shows the key role played by the 13 LOX pathway in RES signaling in the tobacco HR.

In plants, the production of lipid oxidation compounds, known as oxylipins, is activated in response to various stress conditions including wounding and insect and pathogen attacks (Blée, 2002; Howe and Schilmiller, 2002; Weber, 2002; Farmer et al., 2003). The incorporation of molecular oxygen into membrane polyunsaturated fatty acids (PUFAs) is at the origin of the oxylipin pathways leading to a wide array of bioactive metabolites, most of them being involved in signaling (Feussner and Wasternack, 2002). On the one hand, enzymes such as lipoxygenases (LOXs; Feussner and Wasternack, 2002) and α-dioxygenases (Hamberg et al., 2005) are involved in the initial steps of the lipid peroxidation. The metabolic routes for lipid hydroperoxide catabolism are then diverging and are numerous (Blée, 2002; Feussner and Wasternack, 2002; Howe and Schilmiller, 2002; Weber, 2002; Farmer et al., 2003). Using genetic approaches, complex signaling pathways were unraveled, as demonstrated for example for the jasmonate (JA)/oxo-phytodienoic acid (OPDA) pathway (Stintzi et al., 2001). On the other hand, it has now been demonstrated that free radical-mediated lipid peroxidation by reactive oxygen species (ROS) is also at the origin of bioactive oxylipins (Mueller, 2004). Independently from their origin, the biochemical data led to distinguish two classes of bioactive oxylipins, according to their electrophile chemical reactivity. JA, mono-, di-, and tri-hydroxy fatty acids, as well as D_1-, E_1-, and F_1-phytoprostanes, for example, belong to the class of the nonreactive compounds (Mueller, 2004). Their biological activity can be ascribed to the activation of putative receptors that have not yet been described in plants, preceded (or not) by an enzymatic modification, as observed for the obligatory conjugation of JA with Ile (Staswick and Tiryaki, 2004). The other class of metabolites is constituted by the

[1] Present address: Gene Expression Laboratory, Plant Molecular Biology, University of Lausanne, Biophore Building, 1015 Lausanne, Switzerland.

* Corresponding author; e-mail ctriantaphylid@cea.fr; fax 33–4–42–25–26–25.

The author responsible for distribution of materials integral to the findings presented in this article in accordance with the policy described in the Instructions for Authors (www.plantphysiol.org) is: Christian Triantaphylidès (ctriantaphylid@cea.fr).

Article, publication date, and citation information can be found at www.plantphysiol.org/cgi/doi/10.1104/pp.105.074690.

electrophile compounds that can bind spontaneously to cellular nucleophiles, including thiol and amino groups of peptides and proteins. The common structures characterizing these reactive electrophile species (RES) are described in Figure 1, together with one example of a Michaël-type reaction with the most abundant cellular thiol, glutathione (GSH). Oxylipin RES include, in a first group, compounds arising from modifications of the hydroperoxide function and having retained the full fatty acid moiety. Among these compounds, many oxylipins are produced enzymatically (Feussner and Wasternack, 2002), such as conjugated keto fatty acids, epoxy fatty acids, ketols, and OPDA; others are obtained by ROS action (Mueller, 2004), such as cyclopentenone phytoprostanes. A second group of RES compounds is issued from the cleavage of the hydroperoxide fatty acid backbone, leading enzymatically (Feussner and Wasternack, 2002) to products such as nonenal and hexenal, at the origin of green leaves volatiles (GLVs), and by the action of ROS to products such as malondialdehyde (Weber et al., 2004) and 4-hydroxy-nonenal (4-HNE; Schneider et al., 2001).

The fate of this wide array of RES in cells is, at least partly, linked to the RES conjugation with thiol-containing biomolecules such as GSH. In animals, various RES, including cyclopentenone prostaglandines and phenyl propanoids issued from plants, are known to add in vivo to GSH (Hayes and McLellan, 1999; Dinkova-Kostova, 2002) and proteins (Ceaser et al., 2004) and to activate cellular responses. Indeed, whereas at high doses RES can be carcinogens, at lower doses they are able to induce the protective anticarcinogenic enzymes of the phase 2 (Dinkova-Kostova, 2002; Itoh et al., 2004; Xu et al., 2005). Some RES conjugates to GSH issued from the arachidonate pathway, such as leucotriene C_4 and 5-oxo-7glutathionyl-8,11,14-eicosatrienoic acid, were shown to be biologically active compounds (Bowers et al., 2000). In addition, many proteins can be regulated by covalent conjugation to RES, including transcription factors such as NFκ-B (Cernuda-Morollon et al., 2001), c-Jun (Perez-Sala et al., 2003), Nrf2-Keap1 (Itoh et al., 2004; Levonen et al., 2004), and PPARγ (Shiraki et al., 2005).

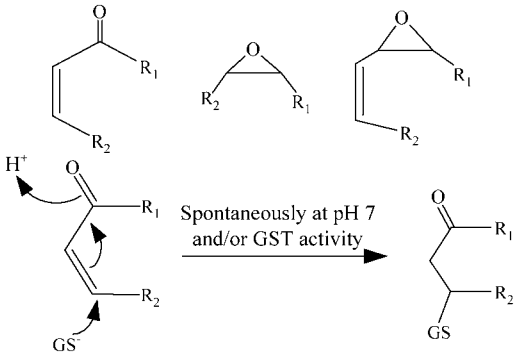

Figure 1. RES. Minimum structures of RES and the 1,4 Michaël addition reaction of GSH on α,β-unsaturated carbonyl compounds.

In plants, the application of RES to leaf tissue was also shown to lead to the induction of GSTs and to a plethora of defense responses (Vollenweider et al., 2000; Weber, 2002; Almeras et al., 2003; Farmer et al., 2003; Weber et al., 2004). The data issued from the transcriptomic analyses indicate that the RES response can be considered as part of the plant response to insect and pathogen attacks (Farmer et al., 2003). At high doses, a rapid cell death has also been reported (Vollenweider et al., 2000; Davoine et al., 2005). We have shown in addition that, under these conditions, oxylipin RES adducts to GSH are produced readily in conjunction with GSH consumption (Davoine et al., 2005). However, oxylipin RES addition to GSH or to proteins under physiological conditions has not yet been reported.

In plant-pathogen interactions, a major source of resistance is related to the development of the hypersensitive response (HR), characterized by the induction of a rapid programmed cell death at the site of infection (Heath, 2000; Greenberg and Yao, 2004). During the course of our studies, we have initially investigated the oxylipin metabolism in cryptogein-elicited tobacco (*Nicotiana tabacum*) leaves, taken as a model of HR (Rustérucci et al., 1999). We have shown that a massive production of 9 LOX metabolites is occurring, in parallel with cell death, involving the induction of transcripts and activities of both galactolipases and 9 LOX and leading to the massive consumption of chloroplastic PUFAs (Rustérucci et al., 1999; Cacas et al., 2005). With the production of JA, the 13 LOX metabolism was also demonstrated as being early involved in tobacco leaves infected with an avirulent strain of *Pseudomonas syringae* pv *phaseolicola* (Kenton et al., 1999). Indeed, both 9 LOX and 13 LOX processes appear to be involved during avirulent pathogen-plant interactions (Blée, 2002; Gobel et al., 2003). In the cryptogein-elicited tobacco model, we additionally showed that the 9 LOX metabolism is exacerbated when the leaves are incubated in the dark (Montillet et al., 2005). Under these conditions, the profiling of the upstream oxylipins (Montillet et al., 2004) indicates that the ratio of product accumulation issued from the 9 LOX-, 13 LOX-, and ROS-mediated lipid peroxidation is 5:1:0.8, respectively (Montillet et al., 2005). Thus, this model appears perfectly suited to investigate the fate of free fatty acid hydroperoxides and derived RES in HR cell death.

We have established in previous experiments that the infiltration at high doses (5 mM) of the upstream oxylipin RES, 13 and 9 keto octadecadien(trien)oic acids [KOD(Tr)E] in healthy tobacco leaves induced tissue necrosis and afforded the expected keto adducts to GSH (Davoine et al., 2005). Quantification of the latter compounds was based on HPLC coupled with tandem mass spectrometry (HPLC-MS^2) techniques, taking advantage of the loss of a glutamyl moiety from the pseudo molecular ion upon collision-induced fragmentation. The analysis was also extended to other oxylipin RES adducts to GSH. Thanks to this established

methodology, we have investigated in this work the production of oxylipin RES adducts to GSH during the development of cryptogein-induced HR of tobacco leaves. Interestingly, our data show that, although the 9 LOX oxylipin metabolism is highly activated, the major oxylipin-GSH adducts are arising from products of the downstream 13 LOX metabolism. The results indicate that the 9 LOX oxylipin pathway does not produce massively oxylipin RES, which could have been involved in HR cell death, and reveal the role of the 13 LOX pathway at the origin of oxylipin RES involved in signaling.

RESULTS

Nonspecific Conjugation of Oxylipin RES to GSH

Infiltration of tobacco leaves with KOD(Tr)E (5 mM) led to cell death after 6 h of incubation and to the corresponding GSH adduct production accompanied by GSH depletion (Davoine et al., 2005). Under the same conditions, the infiltration of the two naturally occurring oxylipin alkenals, trans-2-hexenal and trans-2-nonenal, did not lead to the development of the necrotic symptoms. Analysis of the water-soluble compounds demonstrated a decrease in GSH level (approximately 60%; Table I) similar to that observed upon infiltration of KOD(Tr)E (Davoine et al., 2005). In addition, unambiguous evidence was obtained for production of GSH adducts, characterized by HPLC-MS^2 and quantified in the multiple reaction monitoring (MRM) mode. Surprisingly, in planta, the GSH adducts to both 2-hexenal and 2-nonenal were obtained as their corresponding alcohols, 1-hexanol-3-GSH (Fig. 2) and 1-nonanol-3-GSH, respectively (Table I). These results indicated a carbonyl group reducing activity, likely to be mediated by an alcohol dehydrogenase (ADH), which is not operating on keto fatty acids and other long chain oxylipin RES (Davoine et al., 2005). It should be emphasized that the reduction occurs on the adducts. Indeed, the hydroxyl derivatives resulting from the reduction of the aldehydes are far less reactive and cannot undergo the favored 1,4 Michaël addition of α,β-unsaturated aldehydes. In noninfiltrated leaves, GSH conjugates were not observed, whereas in mock-infiltrated leaves some specific conjugates were produced at very low levels (data not shown), including 1-hexanol-3-GSH, indicating a wounding signature. In a second series of experiments, two non-naturally occurring RES, methyl vinyl ketone (MVK) and acrolein, were applied as volatile compounds. After 15 h of incubation, the adducts were detected as their reduced derivatives 2-butanol-4-GSH and 1-propanol-3-GSH, respectively (Table I). For each tested compound, an approximately 35% decrease in GSH content was observed but was not correlated to a necrosis development. These results show that the conjugation of RES to GSH in planta is nonspecific, occurring whatever the structure of the RES. The process inducing cell death is, on the contrary, dependent on the nature of the RES and occurs at least with long chain fatty acid RES (Davoine et al., 2005).

Oxylipin-GSH Adducts in the Cryptogein-Induced HR

To investigate whether GSH adducts could be generated during the HR, cryptogein-elicited leaves were incubated for 36 h for a full necrosis development and the soluble extracts were analyzed by HPLC-MS^2. We first used the neutral loss mode, which allows the detection of all compounds losing a glutamyl moiety (−129 D) characteristic of the adducts to GSH (Davoine et al., 2005). The typical chromatogram, described in Figure 3A, is expected to show all the soluble adducts to GSH. Accordingly, GSH (peak 4) and oxidized GSH (GSSG; peak 2) were characterized together with 1-hexanol-3-GSH adduct (peak 6). A series of other peaks could be observed that corresponds to GSH adducts produced in lesser amounts. In extracts from control leaves, only the presence of GSH and GSSG could be observed. These results showed that the GSH adducts in elicited leaves are complex mixtures.

Well-defined oxylipin adducts to GSH were more specifically searched and quantified during the time course of HR development by specific MRM analyses. Searching for upstream oxylipin metabolites, we examined at first the 600→471 transition corresponding to KOTrE-GSH and isobaric compounds (Fig. 3B). We have determined that 9- and 13-KOTrE-GSH were very

Table I. *Aspecific production of RES-GSH adducts and reduction of adducts of low molecular weight in tobacco leaves*

Leaves were either treated by the volatile acrolein or MVK or infiltrated by 2-hexenal or 2-nonenal, as indicated in "Materials and Methods." RES-GSH adducts were analyzed by electrospray ionization HPLC-MS^2. For each compound, the *m/z* transition corresponding to the RES-GSH adduct analyzed is indicated. The decrease in the total GSH content and the relative adduct levels are provided. It is noteworthy that contrary to the leaf infiltration of high molecular weight oxylipins for which the GSH adducts were obtained as expected (Davoine et al., 2005), the corresponding low molecular weight adducts are produced as reduced compounds. Results are expressed as mean ± SD of two to three experiments.

Infiltrated Molecules	Corresponding Adduct Mass Transition	Retention Time	GSH Decrease	GSH Adducts
	m/z	*min*	*%*	*% of GSH decrease*
Acrolein	366→237 [CH_2(OH)-CH_2-CH_2-GSH + H^+]	6.5	35.9 ± 1.8	36.5 ± 8
MVK	380→251 [CH_3-CH_2(OH)-CH_2-CH_2-GSH + H^+]	9.9	36.5 ± 2.5	51.2 ± 3.1
2-Hexenal	408→279 [1-hexanol-3-GSH + H^+]	14.6	54.2 ± 2.4	75.3 ± 6.7
2-Nonenal	450→381 [1-nonanol-3-GSH + H^+]	25.0	61.6 ± 0.1	39.5 ± 0.3

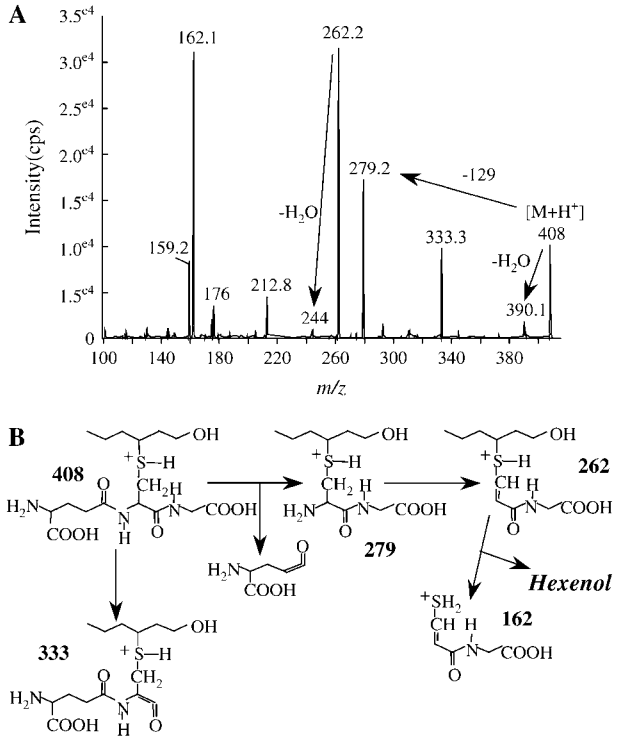

Figure 2. MS analysis of 1-hexanol-3-GSH. A, Positive ion MS^2 analysis after reversed phase HPLC separation of 1-hexanol-3-GSH prepared nonenzymatically by incubation of 2-hexenal with GSH followed by reduction with $NaBH_4$, as described in "Materials and Methods." B, Analysis of the main fragmentations; a special attention will be given to the neutral loss of the glutamyl moiety (−129 D), which is used to investigate the adducts to GSH (see Fig. 3A; Davoine et al., 2005).

minor adducts (35 and 42 pmol g^{-1} dry weight [DW] at 36 h, respectively) as compared to 12-oxo-phytodienoic acid (12-OPDA)-GSH (2–3 nmol g^{-1} DW) and to another nonidentified product. Definitive identification of 12-OPDA-GSH was inferred from coelution with authentic standards under HPLC conditions allowing separation of two diastereoisomeric forms (data not shown). The time-course evolution of the levels of 12-OPDA-GSH and of the estimated cumulated levels of the other compounds is provided in Figure 4, A and B, respectively. The kinetics of accumulation are similar, biphasic, and peak 24 h postinoculation. Searching for KODE-GSH adducts and isobaric compounds, we examined the 602→473 transitions. Three compounds satisfied the MS criteria but could not be identified as KODE adducts on the basis of their retention times (Davoine et al., 2005). In addition, these isobaric compounds to KODE-GSH (mass-to-charge ratio [*m/z*] 602) could not be reduced by $NaBH_4$. Such results indicated that they might be hydroxy compounds, as observed for alkenal adducts. We showed that they did not arise from the reduction of KOTrE-GSH adducts by preparing the corresponding hydroxy adducts via $NaBH_4$ reduction. The estimated cumulated amounts of these compounds reached 10.8 nmol g^{-1} DW, 24 h postinoculation (Fig. 4B). We have searched additionally for the following specific transitions: *m/z* 616→487 and 618→489 corresponding to keto-epoxy-octadecadien (trien)oic acid adducts and their respective structural isomers (Davoine et al., 2005). Two and three compounds fulfill the MS criteria, respectively, but we were not able to assign their structure to a known oxylipin adduct. The GSH adducts with the 616→487 transition are faintly observed while, during the time-course evolution, the estimated cumulated amounts for the 618→489 transitions peaked at 2.2 nmol g^{-1} DW (Fig. 4B). The main adduct in cryptogein-elicited leaves was 1-hexanol-3-GSH, characterized by the *m/z* 408→279 transition and its retention time (Fig. 3C). A full MS^2 fragmentation spectrum could be recorded and was found to be identical to that of the reduced GSH adduct obtained upon incubation with hexenal (Fig. 2). This compound accumulated up to a concentration of 71.5 nmol g^{-1} DW between 30 and 36 h, and

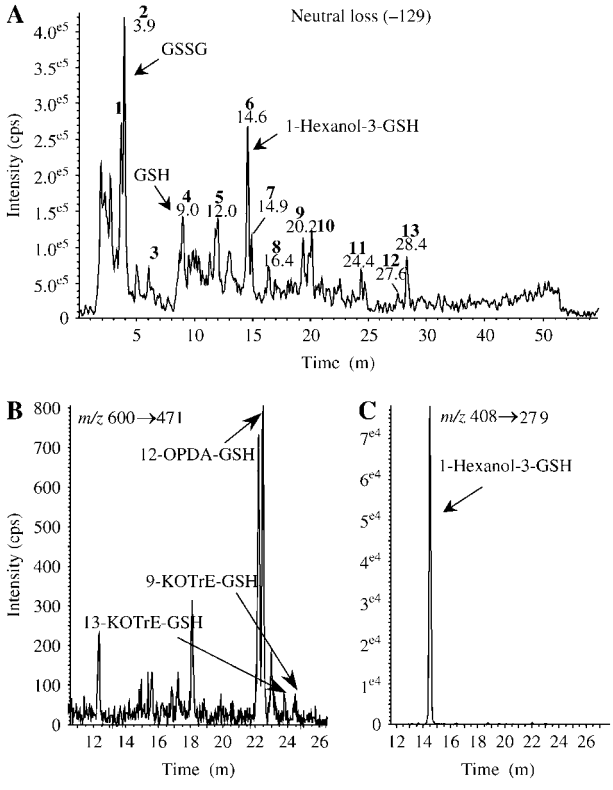

Figure 3. HPLC-MS^2 chromatograms of oxylipin RES adducts to GSH from cryptogein-elicited tobacco leaves. Analysis of water-soluble extracts from cryptogein-elicited leaves after 36 h of incubation. A, Mass spectrometry analysis in the neutral loss mode (corresponding to the glutamyl moiety loss; −129 D); peak 2 corresponds to GSSG, peak 4 to GSH, and peak 6 to 1-hexanol-3-GSH; the other peaks correspond to compounds undergoing loss of 129 mass units upon collision-induced fragmentation and likely to be other nonidentified GSH adducts. B, Mass spectrometry analysis in the MRM mode of KOTrE-GSH and isobaric GSH adducts, including 12-OPDA-GSH (*m/z* 600→471). C, Mass spectrometry analysis by the MRM mode of 1-hexanol-3-GSH (*m/z* 408→279).

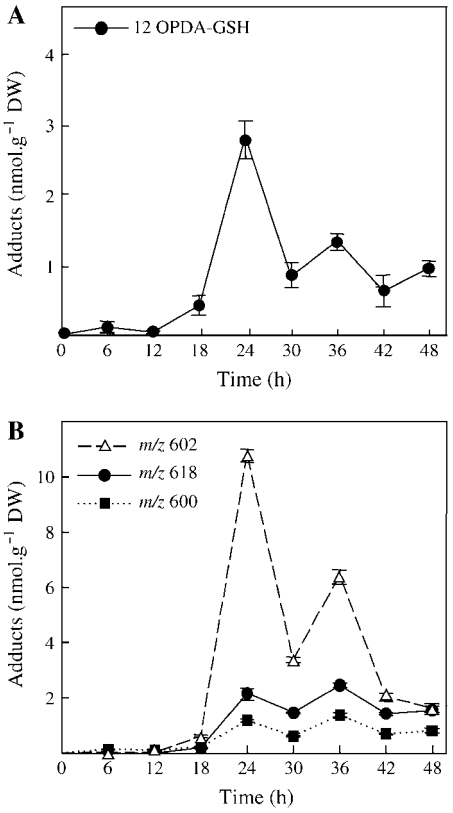

Figure 4. Time-course analysis of high molecular weight conjugated oxylipins to GSH in cryptogein-elicited tobacco leaves. A, Changes in the levels of 12-OPDA adduct to GSH. B, Levels of the estimated cumulated amounts of unidentified oxylipin adducts to GSH, isobaric to KODE (*m/z* 602→473), to keto-epoxy-octadecadienoic acid (*m/z* 618→489), and to KOTrE (*m/z* 600→471) with the exception of 12-OPDA. Results are expressed as mean ± SD from three experiments.

this level decreased thereafter (Fig. 5A). Analysis of the 450→381 transition showed that 2-nonenol-GSH adduct is produced at a low level that peaked at 30 h (maximum accumulation, 0.29 nmol g^{-1} DW) and then decreased (Fig. 5B). Finally, we quantified the GSH adduct to 4-HNE characterized by the specific transitions *m/z* 464→308, 464→233, and 464→179 (Völkel et al., 2005). Contrary to the time-course accumulation of the previous compounds that all peaked and decreased in the late stage of HR development, increase in the level of this adduct was continuous after 18 to 24 h, reaching 22 nmol g^{-1} DW after 48 h of incubation (Fig. 5C).

GSH Consumption and Induction of GST in Cryptogein-Induced HR

We then investigated the changes in GSH levels to correlate them with the production of adducts. In the cryptogein-elicited leaves, we have observed an important consumption of the total GSH content (reduced and bounded GSH as disulfide; see Fig. 6A), which starts with the appearance of the necrotic HR symptoms and the production of oxylipin adducts to GSH, such as 12-OPDA-GSH (Fig. 4A). However, the accumulation of adducts is transient (Fig. 5A), and at their maximum the oxylipin adducts represented only 6% of total GSH consumption.

At physiological pH, conjugation of RES to GSH can occur spontaneously but is enhanced through GST catalysis (Coleman et al., 1997; Dinkova-Kostova, 2002).

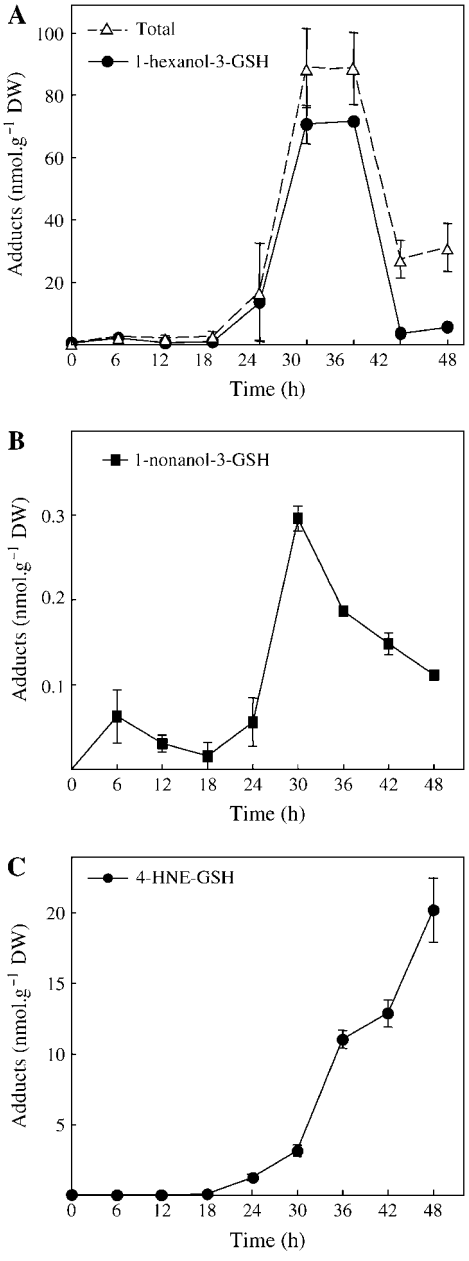

Figure 5. Time-course analysis of conjugated oxylipins to GSH in cryptogein-elicited tobacco leaves. A, Comparison in the level changes of the estimated cumulated amounts of total oxylipin adducts to GSH and of 1-hexanol-3-GSH. B, Changes in the levels of 1-nonanol-3-GSH. C, Accumulation levels of 4-HNE-GSH. Results are mean ± SD from three experiments.

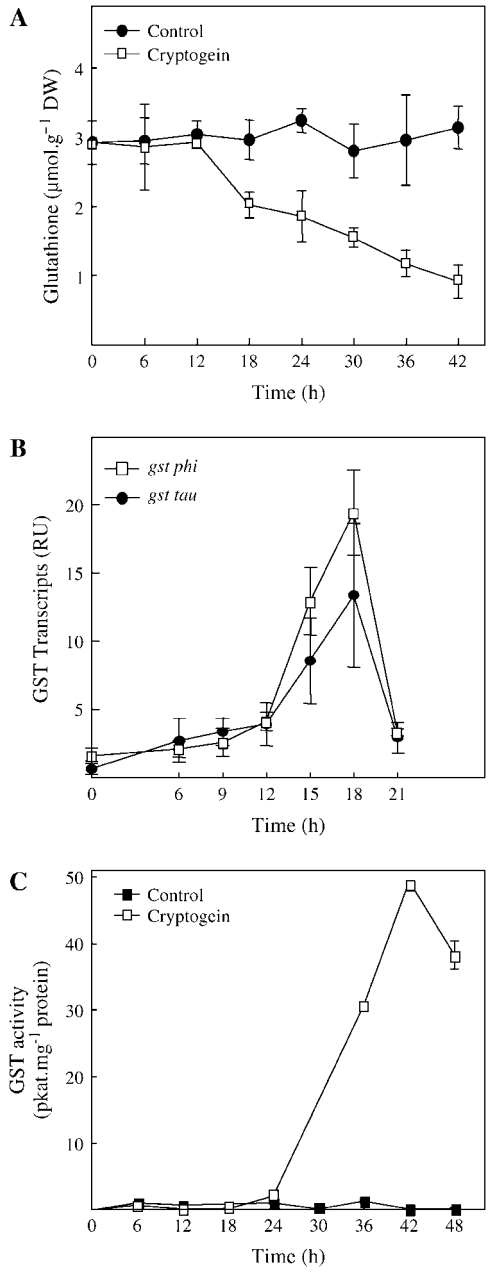

Figure 6. Time-course analysis of GSH levels, of GST transcripts, and activity in cryptogein-elicited tobacco leaves. A, Changes in the level of total GSH (free and bounded in disulfide bridges) in cryptogein-elicited leaves as compared to control. B, Changes in the transcript level accumulation of tobacco *gsts* from the classes Tau and Phi in the elicited leaves, as measured by relative RT-PCR and expressed as relative units (RU). C, Evolution of the GST activity in the elicited leaves as compared to control. See "Materials and Methods" for the experimental procedures. Results are mean ± SD from three experiments.

Different classes of GSTs are able to detoxify a wide spectrum of xenobiotic and endobiotic compounds by conjugation to GSH (Dixon et al., 2002). We have investigated in this context the accumulation of transcripts of tobacco genes from two classes of specific plant GSTs, *gst tau* and *phi*, both being known for their inducibility by biotic and abiotic stresses (Dixon et al., 2002). Our results show that both transcripts are induced 12 h postinoculation with the onset of the symptoms and peaked at 18 h (Fig. 6B). The transcript accumulation is accompanied by the increase of GST activity, as evaluated by the 1-chloro-2,4-dinitrobenzene (CDNB) assay (Fig. 6C). The increase in activity occurred with a delay of 12 h, as compared to the transcript induction, and peaked at 42 h postinoculation. Since 12-OPDA-GSH was observed earlier during the tobacco HR, as soon as 18 h postinoculation (Fig. 3A), these results indicate that the oxylipin conjugation to GSH could occur spontaneously, at least initially, and then could also be enhanced thanks to GST catalysis.

DISCUSSION

We have noticed from this and our previous data (Davoine et al., 2005) that RES conjugation to GSH is facile and, similarly to mammalian cells (Levonen et al., 2004; Shiraki et al., 2005), appears as a nonspecific process. Obviously, the identification of particular RES adducts under physiological conditions should be considered as an evidence for the specific production of the corresponding RES. We show that specific oxylipin RES conjugates to GSH accumulate in tobacco tissues developing the HR. Taking advantage of the HPLC-MS^2 techniques, we have observed that, in cryptogein-elicited tobacco leaves: (1) upstream oxylipin-GSH adducts, such as keto adducts, are minor; (2) many other compounds, including adducts to oxylipins having incorporated a second oxygen atom (*m/z* 616 and 618), are generated at low levels; (3) 1-hexanol-3-GSH, the most abundant adduct (71.5 nmol g^{-1} DW), accumulates transiently together with 12-OPDA-GSH at levels compatible with signaling, both being issued from the 13 LOX pathway; (4) 4-HNE-GSH, a marker of ROS production, accumulates in the late phase of HR; and (5) the synthesis of the adducts is associated with the decrease in total GSH levels and the appearance of the necrotic symptoms.

In response to avirulent plant pathogens, the activation of both 9 and 13 LOX pathways is now a well-established process, involved in signaling and in HR cell death execution. Both processes are accompanied by ROS-mediated lipid peroxidation of membranes (Cacas et al., 2005). In cryptogein-elicited leaves, the PUFAs of chloroplastic membranes are massively consumed (Rustérucci et al., 1999), and, after 30 h of incubation in the dark, the upstream oxylipin assay (Montillet et al., 2004) shows that the 9 and 13 LOX metabolites accumulate at approximately 2,500 and approximately 500 nmol g^{-1} DW, respectively, whereas the ROS-dependent lipid hydroperoxides at approximately 400 nmol g^{-1} DW (Montillet et al., 2005). Interestingly, in this model, the major oxylipin RES adducts to GSH are issued from the 13 LOX pathway, whereas the corresponding RES adducts from the 9 LOX pathway are observed only at trace levels. The

accumulation of 12-OPDA-GSH provides the first strong support for the role played by the 13 LOX pathway in the production of oxylipin RES. This proposal is strengthened by the observation of the accumulation of 1-hexanol-3-GSH. The formation of this compound can be explained by the presence of a hydroperoxide lyase (HPL) activity (Hong et al., 2004) that cleaves the 13 hydroperoxide of the 18:3 fatty acid into cis-3-hexenal, which after isomerization into trans-2-hexenal (Feussner and Wasternack, 2002) adds to GSH. The reduction of the adduct leads finally to the production of 1-hexanol-3-GSH. Comparatively, 1-nonanol-3-GSH, which is issued similarly from the production of 2-nonenal via HPL-catalyzed cleavage of the 9 hydroperoxide of the 18:2 fatty acid, accumulates at much lower levels. Taking into account the respective levels of 18:3 to 18:2 (approximately 4:1) and of 13 to 9 LOX metabolites (approximately 1:5) in the elicited leaves (Rustérucci et al., 1999; Montillet et al., 2005), it can be anticipated that the 13 hydroperoxide of the 18:3 and the 9 hydroperoxide of the 18:2 accumulate at comparable levels. The observation of a 250:1 ratio of the 1-hexanol-3-GSH to 1-nonanol-3-GSH levels (Fig. 5, A and B), which likely reflects the level of aldehydes because the GSH conjugation reaction is not specific, strongly indicates that the tobacco HPL activity is highly 13 specific. Accordingly, a 13 HPL enzymatic activity was described in tomato (*Lycopersicon esculentum*) that does not operate on the 9 hydroperoxides; exhibits a strong preference for the 13 hydroperoxide of 18:3 fatty acid, as compared to 18:2; and leads to the specific production of 2-hexenal (Howe et al., 2000). The accumulation of the 1-hexanol-3-GSH adduct could be explained by a similar specificity of the tobacco HPL. In accordance with this hypothesis, 3-hexenol and 3-hexenyl acetate were identified as the main GLVs produced by cryptogein-elicited leaves (data not shown). We have also noticed differences in the kinetics of accumulation of 12-OPDA-GSH and 1-hexanol-3-GSH, the former peaking before the latter. Recent genetic evidences were provided in tobacco showing that the fatty acid hydroperoxide substrates required for the biosynthesis of JA and GLVs are supplied by separate 13 LOXs (Halitschke et al., 2004). Thus, our data are in the direct line of such observations. In addition to this, the 9- and 13-KOTrE-GSH adducts were observed only at trace levels, indicating that the tobacco LOXs are not very efficient in the transformation of fatty acid hydroperoxides into keto fatty acids, as generally proposed (Feussner and Wasternack, 2002). Finally, among the RES adducts accumulating within ranges of 10 to 20 nmol g^{-1} DW, we have also identified 4-HNE-GSH, confirming that many processes can be at the origin of RES. Indeed, 4-HNE is the result of the double peroxidation of 18:2 fatty acid at the 9 and 13 positions, by both action of LOXs and ROS (Schneider et al., 2001). Such a production shows that ROS can also be, together with LOXs, at the origin of oxylipin RES (Mueller, 2004). Compared to the other adducts, the accumulation of 4-HNE-GSH appears delayed, indicating a significant degradation of membrane fatty acids in the late phase of HR development.

Considering the fate of fatty acid hydroperoxides during the tobacco leaf HR, we suggest, as outlined in Figure 7, that on the one hand, the upstream products of the 9 LOX metabolism accumulate massively and could lead to plant cell death but through mechanisms that are not involving their massive transformation into oxylipin RES followed by their addition to GSH. For example, a direct covalent modification of protein residues by lipid hydroperoxide can be proposed among the possible mechanisms explaining their action (Kawai et al., 2004). On the other hand, the 13 LOX metabolism produces endogenous downstream RES, such as 12-OPDA and 2-hexenal, playing both a role in signaling (Bate and Rothstein, 1998; Stintzi et al., 2001; Howe and Schilmiller, 2002; Farmer et al., 2003) and accumulating as 12-OPDA-GSH and as 1-hexanol-3-GSH, respectively. Consistent with their role in signaling, it is noteworthy that, in the tobacco HR, the level of JA (Kenton et al., 1999) is very similar to the accumulation level of these compounds. In addition, it was proposed that part of the transcription response induced by 12-OPDA is related to its electrophilic properties (Stintzi et al., 2001). Thus, our results confirm this assumption and strongly indicate that 2-hexenal is also acting in signaling similarly. Whether the observed tobacco 13 specificity in the downstream RES production and leading to GSH adducts during HR can be extended to other species is an open question.

In vivo RES conjugation to GSH may occur both spontaneously and through GST catalysis (Coleman et al., 1997; Dinkova-Kostova, 2002). GSTs are known to be induced by electrophile herbicides (Coleman et al., 1997) and also by oxylipin RES (Vollenweider

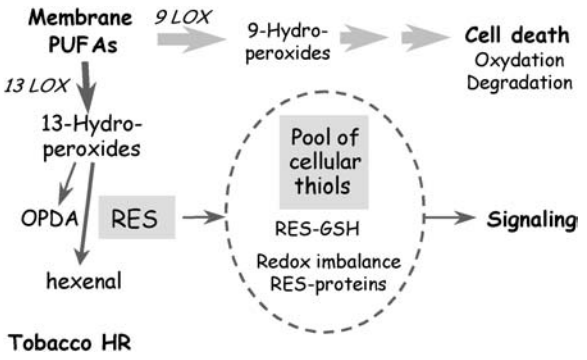

Figure 7. LOX pathways in the tobacco HR. Hypothetical scheme depicting the role of oxylipin RES produced during cryptogein-induced tobacco leaf HR: (1) the production of the fatty acid 9-hydroperoxides is at the origin of cell death processes (Rustérucci et al., 1999; Cacas et al., 2005) that do not include massive production of 9-specific oxylipin RES and conjugation to GSH; and (2) the 13 LOX pathway produces downstream oxylipin RES involved in the signaling of the response (Stintzi et al., 2001; Farmer et al., 2003). These oxylipin RES may add to GSH, change the redox balance, and add to proteins including putative transcription factors.

et al., 2000). In the cryptogein-elicited tobacco leaves, we have observed both an accumulation of transcripts of two GST classes and an increase of total GST activity. However, such accumulations are delayed as compared to the production of oxylipin RES adducts. Thus, our result indicates that the conjugation reaction might occur, at least initially, spontaneously and then with the help of GST activity. In mammals, the inactivation of RES by conjugation to GSH is followed by an efficient metabolization either by reduction/oxidation of the RES moiety or by hydrolysis of the tripeptide part, both leading to the production of urinary-excreted metabolites (Alary et al., 2003). In plants, an efficient metabolism could explain, at least in part, the lower concentration of oxylipin adducts that we observed, with respect to GSH depletion. Interestingly, in the elicited leaves, some of the downstream oxylipin RES adducts accumulated as reduced compounds, indicating an ADH activity. Although cells are kept under a strong oxidative stress, such an activity is apparently operating efficiently, consuming thus reduced cofactors. Moreover, upon leaf treatment with 2-hexenal, 2-nonenal, MVK, and acrolein, the corresponding reduced GSH adducts were observed (Table I), whereas infiltration of KOD(Tr)E gave the nonreduced adducts (Davoine et al., 2005). Furthermore, 12-OPDA-GSH (a keto compound) was identified in cryptogein-elicited leaves, and, as a matter of proof, $NaBH_4$ reduction of extracts from keto fatty acid-infiltrated leaves afforded the expected alcohols (data not shown). We can thus suggest that the ADH activity involved in the metabolization of the adducts is operating only on short chain GSH adducts.

In plant tissues, GSH is regarded as a determinant of cellular redox homeostasis (Meyer and Hell, 2005; Mullineaux and Rausch, 2005; Ogawa, 2005). For example, the systemic response to pathogen attack is accompanied by GSH level increase and changes in the redox state, concomitant with defense gene expression (Fodor et al., 1997; Mou et al., 2003). In cryptogein-elicited tobacco leaves, the incubation in the light leads to the inhibition of the HR symptoms (Cacas et al., 2005) and to a similar GSH level increase (data not shown). Conversely, in the dark, we have observed an irreversible decrease of GSH levels, which is correlated with the development of HR cell death. The transient accumulation of oxylipin RES explains only in part such an irreversible decrease (6% at its maximum). Besides, the phenolic metabolism (La Camera et al., 2004) can also contribute similarly to RES production and GSH depletion. In addition, since keto fatty acids applied massively (5 mM) led to leaf tissue necrosis associated with 60% to 70% of GSH consumption, we have earlier hypothesized that the decrease of GSH level might be a factor involved in cell death (Davoine et al., 2005). In this work, we have noticed that the same level of 2-hexenal or 2-nonenal infiltration led to a similar decrease of GSH level but was not accompanied by cell death (Table I). Thus, these data taken together demonstrate that GSH depletion cannot be considered as determinant or an initiation factor leading to cell death, but should only be considered as one of the many events accompanying HR cell death.

In summary, we have observed that the conjugation of oxylipin RES to GSH occurs in parallel with HR cell death in tobacco leaves. The conjugation process is not specific but involves RES issued mainly from the 13 LOX metabolism. The main oxylipin RES identified in this work are not toxic to the cells and, obviously, their conjugation to GSH cannot be considered as a detoxification mechanism as it is for xenobiotics (Coleman et al., 1997). In accordance with previous results on gene expression (Stintzi et al., 2001; Farmer et al., 2003), we suggest that the production of oxylipin RES, and probably of other endobiotic RES, is involved in plant defense signaling via conjugation processes through three nonexclusive mechanisms (Fig. 7). First, it can be proposed that RES conjugates to GSH play a direct role in signaling. Second, RES conjugation participates to some extent to the alteration of pools of cellular reductant thiols and thus to the changes of the cellular redox balance involved in the regulation of plant defense responses (Meyer and Hell; 2005; Mullineaux and Rausch, 2005; Ogawa, 2005). Finally, the production of GSH adducts can be considered only as a part of the conjugation reactions that occur with thiols from proteins (Levonen et al., 2004) and with other cellular nucleophiles. More specifically, and as in mammalian cells, RES conjugation to putative transcription factors could be involved in the control of plant defense-related gene expression.

MATERIALS AND METHODS

Plant Growth and Treatments

Tobacco (*Nicotiana tabacum*) var. Petit Havana plants were grown for 8 to 9 weeks in greenhouses at 80 μmol m^{-2} s^{-1} light radiance with 14/10-h and 25°C/20°C day/night cycles and 70% relative humidity. Excised leaves were treated by the petiole with 10 μL of cryptogein (0.2 mg mL^{-1}) and incubated in the dark as previously described (Rustérucci et al., 1999). Chemicals (5 mM) in 0.5% Tween 80 were infiltrated between secondary leaf veins, applying the syringe tip to epidermis of leaves, and incubation was carried out for 6 h in the dark prior to analysis. For treatments with MVK and acrolein, the volatile compounds (10 μmol) were applied to cotton wicks and placed in sealed glass chambers (23.5 L) with the leaves for 15 h in the dark.

Preparation of GSH Adducts of Keto and Aldehyde RES

GSH adducts [KOD(Tr)E, 2-nonenal, and 2-hexenal] were synthesized as described previously (Davoine et al., 2005). The reaction mixture (5 mL) consisted of 5 mM GSH and 0.5 mM of RES in 20 mM borate buffer, pH 10. To prepare the corresponding alcohols, the reaction mixture was reduced by $NaBH_4$ (Rustérucci et al., 1999) prior to HCl neutralization and extraction.

Determination of GSH and GSH Adduct Levels

Extractions from plant tissue and analyses were described previously (Davoine et al., 2005). Total GSH levels were determined by HPLC analysis after derivatization with monobromobimane. Both qualitative and quantitative analyses of GSH adducts were performed by HPLC associated with a triple quadrupolar API 3000 mass spectrometer (Perkin Elmer-Sciex). All analyses were performed by positive electrospray ionization HPLC-MS^2 and quantifications according to the MRM mode. The response of the mass

spectrometer was calibrated by injecting a solution of synthetic 9-KODE-GSH of known concentration. Levels of unknown oxylipin RES-GSH adducts were evaluated assuming a comparative response with the known isobaric compounds (Davoine et al., 2005).

Relative Reverse Transcription-PCR

Total RNA was extracted from cryptogein-elicited leaves using TRIzol reagent according to the manufacturer's instructions (Invitrogen Life Technologies, SARL). After a DNase treatment (Invitrogen Life Technologies), RNA (1 μg) was reverse transcribed using the first-strand cDNA synthesis kit (Amersham Biosciences) with oligo$(dT)_{18}$ as the primer. Then, the expression study of each of the GST genes, corresponding to classes Phi and Tau and named *gst phi* and *gst tau*, respectively, was carried out using the specific primers 5′-GGC GAT CAA AGT CCA TGG TAG CCC-3′ (sense) and 5′-CCA ATC CCT TAA CCC AAG CTG GCC-3′ (antisense) for *gst phi*, and 5′-TTC AGT GGG CTC TAA AGA TAA GGG CG-3′ (sense) and 5′-GGC TGC AGT TAA TGT ACT CAT CTC-3′ (antisense) for *gst tau*. These primers were designed from conserved and specific domains of a number of aligned GSTs sequences of the classes Phi and Tau, respectively, and thanks to the ClustalW program (http://www.infobiogen.fr). Relative reverse transcription (RT)-PCR was performed by coamplifying the gene of interest (*gst phi*, *gst tau*) with a housekeeping gene corresponding to *gapdh* (glyceraldehyde-3-P dehydrogenase) as internal control. The corresponding fragment of *gapdh* was amplified using degenerate primers (Winge et al., 1997). The PCR was performed according to the manufacturer's instruction (Sigma-Aldrich Chimie SARL) in a final volume (25 μL) containing 0.2 units of Taq polymerase, 200 nM of each primer, 200 μM of each dNTP, and 5 μL of DNA (diluted 50-fold). Amplification was performed for 37 cycles: one cycle at 95°C for 10 min, 35 cycles at 95°C for 30 s, 50°C for 30 s, 72°C for 70 s, and one cycle at 72°C for 10 min. Amplified products were then separated on gel (1.5% agarose in 0.5× Tris-Borate-EDTA buffer) stained with ethidium bromide. The fluorescence signals were integrated with the Scion Imaging Software (http://www.scioncorp.com).

GST Activity

For quantification of GST activity, frozen leaves were ground in mortar and pestle and extracted in 50 mM potassium phosphate, pH 7.2, buffer containing 2 mM dithiothreitol, 0.01% Triton 100-X, 1 mM EDTA, and 8% polyvinylpolypyrrolidone. After filtration on Miracloth and centrifugation (23,220*g*, 30 min at 4°C), the supernatant was used for the GST assay. The assay was performed according to Habig et al. (1974) in a final volume of 1 mL containing 100 μL of extract, 100 μL GSH (10 mM), 10 μL CDNB (100 mM in ethanol), and 790 μL potassium phosphate buffer (50 mM, pH 7.2). The reaction was followed during 10 min at 340 nm. Controls without GSH and CDNB, respectively, were realized to determine the specific GST activity. For each sample, the amount of soluble proteins was determined according to the method of Bradford (1976) using bovine serum albumin as standard. The enzyme activity was expressed in pkat mg^{-1} of proteins. A molar extinction coefficient of 9.6 mM^{-1} cm^{-1} for CDNB was used for the calculations.

Sequence data from this article can be found in the GenBank/EMBL data libraries under accession numbers gi|1170088, gi|232202, gi|416649, and gi|416651.

ACKNOWLEDGMENTS

We thank the GRAP team (CEA Cadarache, DSV-DEVM, France) for the plant culture technical support and Denis Rontein (Librophyt, France) for the gas chromatography-mass spectrometry analyses of the GLVs.

Received November 24, 2005; revised February 8, 2006; accepted February 10, 2006; published February 24, 2006.

LITERATURE CITED

Alary J, Gueraud F, Cravedi JP (2003) Fate of 4-hydroxynonenal in vivo: disposition and metabolic pathways. Mol Aspects Med **24:** 177–187

Almeras E, Stolz S, Vollenweider S, Reymond P, Mene-Saffrane L, Farmer EE (2003) Reactive electrophile species activate defense gene expression in Arabidopsis. Plant J **34:** 205–216

Bate NJ, Rothstein SJ (1998) C6-volatiles derived from the lipoxygenase pathway induce a subset of defense-related genes. Plant J **16:** 561–569

Blée E (2002) Impact of phyto-oxylipins in plant defense. Trends Plant Sci **7:** 315–322

Bowers RC, Hevko J, Henson PM, Murphy RC (2000) A novel glutathione containing eicosanoid (FOG_7) chemotactic for human granulocytes. J Biol Chem **29:** 29931–29934

Bradford MM (1976) A rapid and sensitive method for the quantification of microgram quantities of proteins utilizing the principle of protein-dye binding. Anal Biochem **72:** 248–254

Cacas JL, Vailleau F, Davoine C, Ennar N, Agnel JP, Tronchet M, Ponchet M, Blein JP, Roby D, Triantaphylidès C, et al (2005) The combined action of 9 lipoxygenase and galactolipase is sufficient to bring about programmed cell death during tobacco hypersensitive response. Plant Cell Environ **28:** 1367–1378

Ceaser EK, Moellering DR, Shiva S, Ramachandran A, Landar A, Venkartraman A, Crawford J, Patel R, Dickinson DA, Ulasova E, et al (2004) Mechanisms of signal transduction mediated by oxidized lipids: the role of the electrophile-responsive proteome. Biochem Soc Trans **32:** 151–155

Cernuda-Morollon E, Pineda-Molina E, Canada FJ, Perez-Sala D (2001) 15-Deoxy-delta 12,14-prostaglandin J2 inhibition of NF-kappaB-DNA binding through covalent modification of the p50 subunit. J Biol Chem **276:** 35530–35536

Coleman JOD, Blake-Kalff MMA, Davis ETG (1997) Detoxification of xenobiotics by plants: chemical modification and vacuolar compartmentation. Trends Plant Sci **2:** 144–151

Davoine C, Douki T, Iacazio G, Montillet JL, Triantaphylidès C (2005) Conjugation of keto fatty acids to glutathione in plant tissues. Characterisation and quantification by HPLC-tandem mass spectrometry. Anal Chem **77:** 7366–7372

Dinkova-Kostova AT (2002) Protection against cancer by plant phenylpropenoids: induction of mammalian anticarcinogenic enzymes. Mini Rev Med Chem **2:** 595–610

Dixon DP, Lapthorn A, Edwards R (2002) Plant glutathione transferases. Genome Biol **3:** REVIEWS3004

Farmer EE, Almeras E, Krishnamurthy V (2003) Jasmonates and related oxylipins in plant responses to pathogenesis and herbivory. Curr Opin Plant Biol **6:** 372–378

Feussner I, Wasternack C (2002) The lipoxygenase pathway. Annu Rev Plant Biol **53:** 275–297

Fodor J, Gullner G, Adam AL, Barna B, Komives T, Kiraly Z (1997) Local and systemic responses of antioxidants to tobacco mosaic virus infection and to salicylic acid in tobacco (role in systemic acquired resistance). Plant Physiol **114:** 1443–1451

Gobel C, Feussner I, Rosahl S (2003) Lipid peroxidation during the hypersensitive response in potato in the absence of 9-lipoxygenases. J Biol Chem **278:** 52834–52840

Greenberg JT, Yao N (2004) The role and regulation of programmed cell death in plant-pathogen interactions. Cell Microbiol **6:** 201–211

Habig WH, Pabst MJ, Jakobi WB (1974) Glutathione-*S*-transferases. The first enzymatic step in mercapturic acid formation. J Biol Chem **242:** 5329–5335

Halitschke R, Ziegler J, Keinanen M, Baldwin IT (2004) Silencing of hydroperoxide lyase and allene oxide synthase reveals substrate and defense signaling crosstalk in Nicotiana attenuata. Plant J **40:** 35–46

Hamberg M, Ponce de Leon I, Rodriguez MJ, Castresana C (2005) Alpha-dioxygenases. Biochem Biophys Res Commun **338:** 169–174

Hayes JD, McLellan LI (1999) Glutathione and glutathione-dependent enzymes represent a co-ordinately regulated defence against oxidative stress. Free Radic Res **31:** 273–300

Heath MC (2000) Hypersensitive response-related cell death. Plant Mol Biol **44:** 321–334

Hong M, Zilinskas BA, Knipple DC, Chin CK (2004) cis-3-Hexenal production in tobacco is stimulated by 16-carbon monounsaturated fatty acids. Phytochemistry **65:** 159–168

Howe GA, Lee GI, Itoh A, Li L, DeRocher AE (2000) Cytochrome P450-dependent metabolism of oxylipins in tomato. Cloning and expression of allene oxide synthase and fatty acid hydroperoxide lyase. Plant Physiol **123:** 711–724

Howe GA, Schilmiller AL (2002) Oxylipin metabolism in response to stress. Curr Opin Plant Biol **5:** 230–236

Itoh K, Tong KI, Yamamoto M (2004) Molecular mechanism activating Nrf2-Keap1 pathway in regulation of adaptive response to electrophiles. Free Radic Biol Med **36:** 1208–1213

Kawai Y, Fujii H, Kato Y, Kodama M, Naito M, Uchida K, Osawa T (2004) Esterified lipid hydroperoxide-derived modification of protein: formation of a carboxyalkylamide-type lysine adduct in human atherosclerotic lesions. Biochem Biophys Res Commun **313:** 271–276

Kenton P, Mur LAJ, Atzorn R, Wasternack C, Draper J (1999) Jasmonic acid accumulation in tobacco hypersensitive response lesions. Mol Plant Microbe Interact **12:** 74–78

La Camera S, Gouzerh G, Dhondt S, Hoffmann L, Fritig B, Legrand M, Heitz T (2004) Metabolic reprogramming in plant innate immunity: the contributions of phenylpropanoid and oxylipin pathways. Immunol Rev **198:** 267–284

Levonen AL, Landar A, Ramachandran A, Ceaser EK, Dickinson DA, Zanoni G, Morrow JD, Darley-Usmar VM (2004) Cellular mechanisms of redox cell signalling: role of cysteine modification in controlling antioxidant defences in response to electrophilic lipid oxidation products. Biochem J **378:** 373–382

Meyer AJ, Hell R (2005) Glutathione homeostasis and redox-regulation by sulfhydryl groups. Photosynth Res **86:** 435–457

Montillet JL, Cacas JL, Garnier L, Montané MH, Douki T, Bessoule JJ, Polkowska-Kowalczyk L, Maciejewska U, Agnel JP, Vial A, et al (2004) The upstream oxylipin profile of *Arabidopsis thaliana*. A tool to scan for oxidative stresses. Plant J **40:** 439–451

Montillet JL, Chamnongpol S, Rusterucci C, Dat J, van de Cotte B, Agnel JP, Battesti C, Inze D, Van Breusegem F, Triantaphylides C (2005) Fatty acid hydroperoxides and H_2O_2 in the execution of hypersensitive cell death in tobacco leaves. Plant Physiol **138:** 1516–1526

Mou Z, Fan W, Dong X (2003) Inducers of plant systemic acquired resistance regulate NPR1 function through redox changes. Cell **113:** 935–944

Mueller MJ (2004) Archetype signals in plants: the phytoprostanes. Curr Opin Plant Biol **7:** 441–448

Mullineaux PM, Rausch T (2005) Glutathione, photosynthesis and the redox regulation of stress-responsive gene expression. Photosynth Res **86:** 459–474

Ogawa K (2005) Glutathione-associated regulation of plant growth and stress responses. Antioxid Redox Signal **7:** 973–981

Perez-Sala D, Cernuda-Morollon E, Canada FJ (2003) Molecular basis for the direct inhibition of AP-1 DNA binding by 15-deoxy-delta 12,14-prostaglandin J2. J Biol Chem **278:** 51251–51260

Rustérucci C, Montillet JL, Agnel JP, Battesti C, Alonso B, Knoll A, Bessoule JJ, Etienne P, Suty L, Blein JP, et al (1999) Involvement of lipoxygenase-dependent production of fatty acid hydroperoxides in the development of the hypersensitive cell death induced by cryptogein on tobacco leaves. J Biol Chem **274:** 36446–36455

Schneider C, Tallman KA, Porter NA, Brash AR (2001) Two distinct pathways of formation of 4-hydroxynonenal. Mechanisms of nonenzymatic transformation of the 9- and 13-hydroperoxides of linoleic acid to 4-hydroxyalkenals. J Biol Chem **276:** 20831–20838

Shiraki T, Kamiya N, Shiki S, Kodama TS, Kakizuka A, Jingami H (2005) Alpha,beta-unsaturated ketone is a core moiety of natural ligands for covalent binding to peroxisome proliferator-activated receptor gamma. J Biol Chem **280:** 14145–14153

Staswick PE, Tiryaki I (2004) The oxylipin signal jasmonic acid is activated by an enzyme that conjugates it to isoleucine in Arabidopsis. Plant Cell **16:** 2117–2127

Stintzi A, Weber H, Reymond P, Browse J, Farmer EE (2001) Plant defense in the absence of jasmonic acid: the role of cyclopentenones. Proc Natl Acad Sci USA **98:** 12837–12842

Völkel W, Alvarez-Sanchez R, Weick I, Mally A, Dekant W, Pähler A (2005) Glutathione conjugates of 4-hydroxy-2(E)-nonenal as biomarkers of hepatic oxidative stress-induced lipid peroxidation in rats. Free Radic Biol Med **38:** 1526–1536

Vollenweider S, Weber H, Stolz S, Chetelat A, Farmer EE (2000) Fatty acid ketodienes and fatty acid ketotrienes: Michael addition acceptors that accumulate in wounded and diseased Arabidopsis leaves. Plant J **24:** 467–476

Weber H (2002) Fatty acid-derived signals in plants. Trends Plant Sci **7:** 217–224

Weber H, Chetelat A, Reymond P, Farmer EE (2004) Selective and powerful stress gene expression in Arabidopsis in response to malondialdehyde. Plant J **37:** 877–888

Winge P, Brembu T, Bones AM (1997) Cloning and characterization of rac-like cDNAs from Arabidopsis thaliana. Plant Mol Biol **35:** 483–495

Xu C, Li CY, Kong AN (2005) Induction of phase I, II and III drug metabolism/transport by xenobiotics. Arch Pharm Res **28:** 249–268